Mech. Sci., 17, 415–425, 2026
https://doi.org/10.5194/ms-17-415-2026

Mechanical Sciences
Open Access

Research on milling performance of textured carbide milling cutter based on laser cladding principle

Shucai Yang, Zhe Ning, Xin Tong, and Shiwen Xing

Key Laboratory of Advanced Manufacturing and Intelligent Technology, Ministry of Education, Harbin University of Science and Technology, Harbin, 150080, China

Correspondence: Zhe Ning (18945566223@163.com)

Received: 8 November 2025 – Revised: 16 March 2026 – Accepted: 28 March 2026 – Published: 14 April 2026

Abstract. Traditional laser processing of micro-textures directly impacts the work surface, leading to significant crack propagation and pore formation around textured pits. These defects result in poor surface quality and insufficient hardness, which in turn deteriorate the tool's milling performance and surface hardness. To enhance the surface properties of the texture and improve the milling performance of the ball-end milling cutter, this paper integrates the prefabricated powder-feeding laser cladding method with the laser preparation micro-texture technique to establish a modified textured ball-end milling cutter milling titanium alloy test platform. The milling performance of cemented carbide modified textured ball-end milling cutters, both with and without coating deposition treatment, was investigated. The findings indicate that at an average laser energy density of 70.8 W cm^{-2}, the grain structure on the surface of the modified textured tool has a fine-grain-strengthening effect, enhancing surface hardness and reducing vibration. During milling, aluminum in the coating oxidizes to form an Al2O3 film with a high melting point and solid lubrication properties, effectively lowering the friction coefficient and improving cutting stability. The surface micro-hardness of the modified textured tool increases by approximately 35 %, accompanied by a substantial presence of hard phases within the strengthening layer. As wear progresses, the detachment of these hard phases further decreases the friction coefficient, resulting in an average reduction of frictional force by about 13.1 %. Concurrently, the lifespan of the strengthening layer is extended, which effectively mitigates wear on the rake face of the ball-end milling cutter. Concurrently, the passivation of the tool edge during the cutting process is mitigated, leading to reduced material adhesion phenomenon in the cutting process, which ultimately enhances the machined surface quality of the workpiece. Moreover,the deposition of the coating not only establishes a dense alumina structure that resists wear at the tool–chip interface but also enhances the bonding strength of the tool surface, curbing the formation of built-up edges and promoting better surface roughness in the machining of titanium alloys. Overall, this study achieves a synergistic enhancement of surface wear resistance and cutting performance in cemented carbide tools, providing valuable insights for the efficient machining of difficult-to-cut materials in aerospace and shipbuilding applications.

1 Introduction

Recent tribological and biomimetic studies have demonstrated that micro-pits and protrusions found on the tool surfaces can significantly enhance wear resistance and reduce friction (Sheng et al., 2025). Experimental investigations by numerous scholars have confirmed that the placement and design of surface micro-textures play a crucial role in improving tool cutting performance. Among various fabrication techniques, laser micro-texturing has been widely adopted due to its high controllability, operational simplicity, and efficiency. However, the direct impact of laser energy on the substrate surface often leads to severe crack propagation, resulting in poor surface quality in the textured regions. In contrast, laser cladding technology utilizes a high-energy-density laser beam to melt material and fuse it with the substrate surface, thereby generating a cladding layer with tailored properties (Tan et al., 2020). The integration of laser cladding technology with laser micro-texture preparation can enhance pit

morphology and surrounding surface properties, thereby improving the surface hardness of the tool and its milling performance.

In the current domain of micro-texture on tool surface coatings, Li et al. (2025) and Zhang (2024) applied liquid-phase-assisted laser texturing to a DLC/TiAlN composite coating tool, followed by dry cutting experiments. The findings indicate that the cutting force of the liquid-phase-assisted laser-textured composite coating tools is significantly lower than that of untreated tools, effectively inhibiting wear and coating delamination. Meng (2022) and Zhou (2022) combined laser texturing technology with physical vapor deposition coating technology to treat the surfaces of cemented carbide substrates. Meng (2022) observed that AlCrN coatings formed on laser-pretreated surfaces exhibited a regular fish-scale structure, enhancing the anti-stripping capability of the AlCrN coating. Zhou (2022) observed that composite textured AlCrN-coated tools displayed higher surface hardness and reduced wear compared to non-textured coated tools. Tong et al. (2023a) fabricated micro-textures combined with AlCrN coatings on cemented carbide surfaces; friction and wear tests revealed that the micro-textured coatings positively influenced frictional performance. Li et al. (2023) and Wu et al. (2022) fabricated micro-textures on the flank faces of coated tools and conducted milling experiments. Their results demonstrated that, compared to non-textured coated tools, the textured coated tools significantly reduced milling forces, milling temperatures, friction coefficients, and flank wear.

Laser cladding technology effectively compensates for the inherent deficiencies of the substrate surface, endowing it with superior properties such as high-temperature resistance, wear resistance, and corrosion resistance. Ni et al. (2025) and Wang et al. (2023) investigated the laser cladding coatings on titanium alloy surfaces, focusing on their structural characteristics, wear resistance, and corrosion resistance. The findings indicate that the cladding layer exhibits strong adhesion to the substrate, with hardness values several times greater than that of the substrate, resulting in improved wear resistance and notable corrosion resistance. Similarly, Jie et al. (2022) employed laser cladding to deposit Ni-based alloys onto substrate surfaces; friction and wear testing revealed that numerous fine and uniformly distributed hard phases within the cladding layer acted as supportive frameworks, substantially reducing both the friction coefficient and wear volume. Li et al. (2023) explored the fabrication of high-entropy alloy (HEA) coatings via laser cladding at varying power levels, observing that coatings produced at lower power exhibited uneven hardness distribution, increased surface roughness, and higher friction coefficients, yet maintained commendable wear resistance. Liang et al. (2023) and Huang et al. (2025) investigated the forming quality and dilution rate regulation in laser cladding of high-entropy alloy coatings. Their studies demonstrate that optimizing process parameters, including laser power, scanning speed, and powder feeding rate, can effectively decrease the dilution rate, markedly enhance the coating's forming quality, and minimize coating defects. Furthermore, Xing et al. (2024) developed modified micro-textures through laser cladding, analyzing the phase composition and micro-hardness of textured surfaces under varying laser average energy densities, and investigating their friction and wear behaviors.

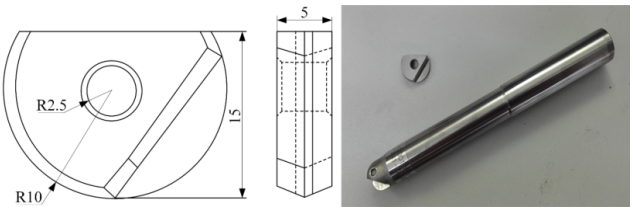

Figure 1. Ball-end milling cutter and its size diagram.

These studies demonstrate that pre-set cladding materials can effectively repair texture defects, enhance surface hardness, and produce modified textures. Specifically, the cladding powder, when pre-applied to the target surface, melts during the laser texturing process to fill pits and inhibit crack propagation, thereby improving surface hardness and wear resistance in the textured regions and enhancing overall tool performance. The existing research mainly focuses on the performance of a single modified textured tool or a textured coating tool. However, there are relatively few studies on the synergistic mechanism between laser cladding modified texture and coating. In this paper, a modified micro-texture structure based on the laser cladding principle is proposed and further forms a synergistic strengthening system with AlCrN coating. This study fabricated both modified and conventional textured ball-end milling cutters, with and without coating deposition, based on optimized texture geometry and process parameters. A titanium alloy milling test platform was established to compare milling force, tool wear, and surface quality, revealing the mechanisms through which modified texture and modified textured coating technologies influence the cutting performance of ball-end milling cutters.

2 Experimental design

2.1 Selection and preparation of test materials

The milling experiment utilized a YG8 cemented carbide ball-end milling cutter with a diameter of 20 mm and a thickness of 5 mm, corresponding to a tool bar dimension of $\Phi 20 \times 141$ mm. The tool bar was fabricated from a cemented carbide rod, as illustrated in Fig. 1.

Prior to laser texturing, the rake face of the ball-end milling cutter is prepared using diamond sandpaper. This treatment enhances the surface's capacity to absorb laser energy, thereby improving the stability and quality of micro-texture formation. Additionally, it strengthens the bonding reliability between the modified layer and the underlying

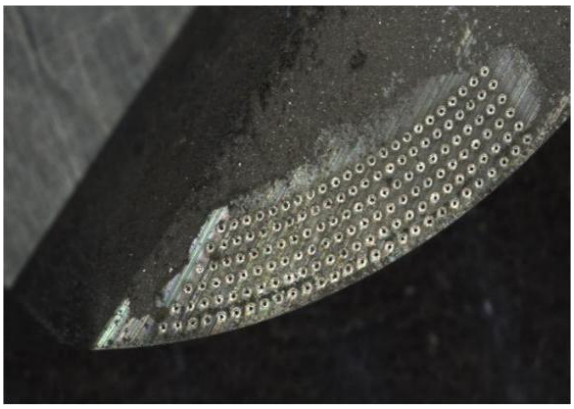

Figure 2. Tool-modified textured surface microstructure diagram.

substrate. Subsequently, the rake face underwent ultrasonic cleaning with a 95 % ethanol solution to eliminate surface oils and contaminants, followed by natural air drying. High-purity cobalt (Co) powder served as the metallic binder, while high-purity spherical cast tungsten carbide (WC) and titanium carbide (TiC) powders, containing trace amounts of aluminum (Al), oxygen (O), and iron (Fe), acted as reinforcing phases. The powders were mixed in a mass ratio of WC : Co : TiC = 78 : 17 : 5 (wt %) (Liang et al., 2021). The mixture was weighed using a precision electronic balance, dried, and then placed in a ball-mill mixer with a ball-to-powder ratio of 5 : 1. Milling was performed for 4 h at 200 rpm to ensure the uniform dispersion of the components.

After determining the micro-texture placement area, the mixed grinding cladding material and anhydrous ethanol were evenly applied to the rake face of the ball-end milling cutter at a powder-to-alcohol ratio of 1 : 0.5. The coated tool was then placed in a dry environment to facilitate the drying of the coating. Micro-textures were fabricated using a Beijing Zhengtian ZTQ-50 fiber laser marking system. The resulting micro-texture morphology is shown in Fig. 2. After processing, the surface of the textured cutter was cleaned with 95 % ethanol to remove any residual powder, followed by ultrasonic cleaning to eliminate impurities remaining in the micro-pits.

The AlCrN coating was selected as the surface coating for the cutting tool. Following the preparation of the modified texture, the AlCrN coating was deposited onto the tool surface using vacuum cathodic arc deposition technology, employing arc evaporation equipment manufactured by Oerlikon Balzers Coatings Co., Ltd.

2.2 Experimental design

In the experiment on modified texture preparation, a five-factor, four-level orthogonal test was designed based on the parameters of laser processing and texture. The five influencing factors included laser power (p), scanning speed (v), number of scanning passes (n), texture spacing (l), and texture diameter (d). Based on the team's previous research findings, four levels were established for each factor, leading to the formulation of the orthogonal experimental scheme, as presented in Table 1. The laser equipment utilized in the experiment had a rated power of 50 W, and the spot diameter (D) was determined by the equation $D = d/2+5$ (μm). Some samples were subsequently coated with AlCrN. The texture of the surface cladding layer formed by the coated cladding material is recorded as group K; the control group without coating was set up to prepare texture, which was recorded as the J group.

To account for the combined effects of laser power and spot diameter, the average energy density of the laser was calculated using Eq. (1), and the energy values for each experimental condition were summarized in Table 1.

$$\overline{W} = \frac{E}{N \cdot S} = \frac{P}{f \cdot S} \tag{1}$$

In the formula, E represents the total energy input of the textured single pit (in J), N denotes the total number of spots surrounding a single pit; S indicates the spot area (in cm^2), f is the laser input frequency (in Hz), and P signifies the laser power (in W).

2.3 Milling test platform construction

In this milling experiment, a VDL-1000E three-axis vertical milling machine, manufactured by Dalian Machine Tool Factory (as depicted in Fig. 3a), was employed. The Ti6Al4V workpiece measured 150 mm in length and 100 mm in width during the milling process. To mitigate the risk of premature tool failure due to damage to the tool tip and to enhance the surface quality of the machined workpiece,a jaw clamp set at a 15° angle was utilized. Based on prior experimental investigations, the machining parameters were established as follows: cutting speed (v) of 140 mm min^{-1}, cutting depth (a_p) of 0.3 mm, feed rate (f) of 0.06 mm per revolution, and a milling stroke length of 150 mm per pass. During milling, horizontal milling is carried out along the length direction of the workpiece. In order to achieve green cutting and to avoid the masking effect of coolant on micro-texture friction reduction, chip storage, and cutting stability – so as to more truly reflect the role of micro-texture in interface friction and wear – lubricant is not used in this experiment (Tatsuya et al., 2009; Wu et al., 2021). A rotary dynamometer was used to capture milling force data. Each tool travels twice to collect a set of data; that is, two 150 mm trips in the length direction, and a total of 50 sets of data are collected for 100 times. To ensure data reliability and to exclude anomalies arising from machine tool vibrations and charge amplifier drift within the data acquisition system, outlier values were identified and removed during data processing. Subsequently, the milling force components along the x, y, and z axes were recorded,

Table 1. Five factors and four levels orthogonal test table (Xing et al., 2024).

Factor	Laser parameters			Texture parameter		Coating	Average laser energy
Serial number	p (%)	v (mm s^{-1})	n	l (µm)	d (µm)		density (W cm^{-2})
K1/J1	75 %	1100	6	130	40	AlCrN	95.5
K2/J2	80 %	1500	9	130	50	Nil	70.8
K3/J3	80 %	1700	8	150	40	AlCrN	101.9
K4/J4	85 %	1100	8	190	50	Nil	75.2
K4/J4	85 %	1100	8	190	50	AlCrN	75.2
K5/J5	85 %	1300	9	170	40	AlCrN	108.3
K5/J5	85 %	1300	9	170	40	Nil	108.3
K6/J6	90 %	1500	7	190	40	AlCrN	114.6

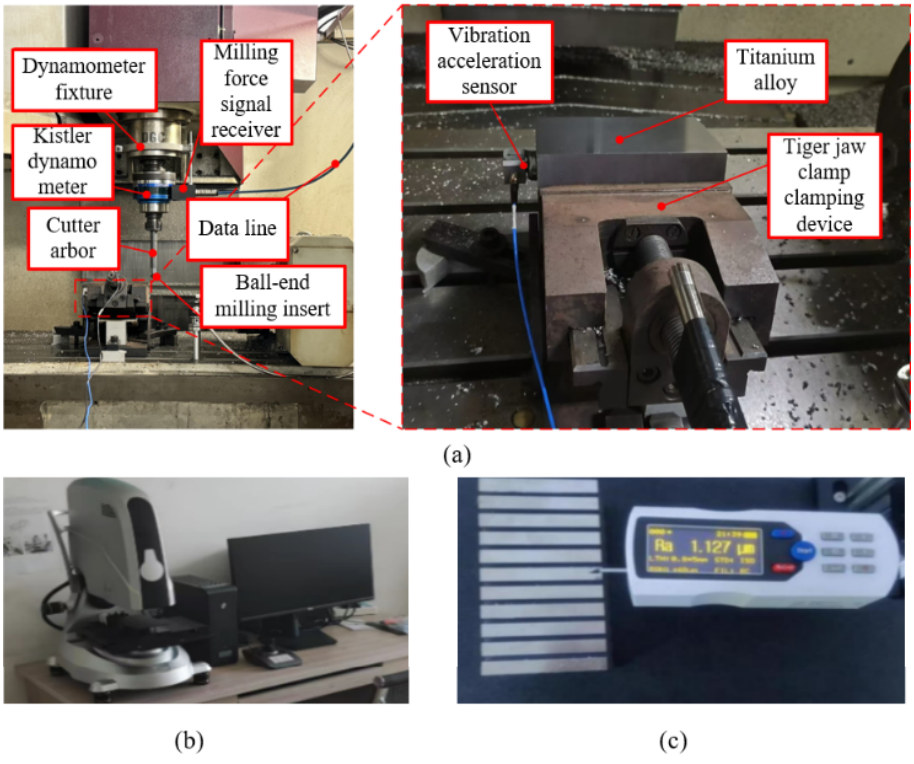

Figure 3. Milling test platform construction. **(a)** Milling test field device diagram. **(b)** Ultra-depth-of-field microscope. **(c)** TR-200 surface roughness meter.

and the resultant force was computed and documented as a data set.

To evaluate the efficacy of the laser-cladding-based modified texture in enhancing the wear resistance of the textured coating on the ball-end milling cutter, wear measurements were conducted on the rake face of the cutter, where the modified texture was applied. Observations were made using an ultra-depth-of-field microscope, consistent with the equipment shown in Fig. 3b. Prior to examination, the rake face was cleaned with alcohol to eliminate adhered chips and contaminants. The wear area was delineated using Image Pro Plus software to identify the maximum wear region, as illustrated in Fig. 3. To enhance measurement accuracy, each tool was assessed three times at different locations within the wear area, and the mean value was calculated to represent the final wear measurement.

To investigate the influence of modified textures fabricated via laser cladding on the surface roughness of titanium alloy machined using a textured coating ball-end milling cutter, surface roughness measurements were conducted following the milling tests. The surface roughness of the titanium alloy was assessed using a TR-200 surface roughness meter, which offers a measurement accuracy of 0.001 µm. The testing apparatus is depicted in Fig. 3c. To ensure the reliability and

accuracy of the results, measurements were taken at three distinct locations on the machined surface, and the average value was calculated.

3 Results and analysis

3.1 Analysis of milling force results for ball-end milling cutters featuring surface-modified textured coatings on cemented carbide

To investigate the variation trend of milling forces throughout the entire cutting process, and ensure the representativeness and differentiation between data points, the average value of 10 data sets (corresponding to 20 cutting cycles) was recorded as a single data point. The milling force values in the range of 40 to 60 cutting passes were selected as the effective average values. The trend of these effective average milling forces is illustrated in Fig. 4.

As depicted in Fig. 4a, when the average laser energy density is set at $70.8\,W\,cm^{-2}$, the modified textured ball-end milling cutter demonstrates the lowest effective average milling force throughout the milling process. In comparison to the corresponding traditional textured ball-end milling cutter, this modified cutter exhibits the most significant reduction in effective average milling force. Moreover, relative to the traditional textured cemented carbide, the surface micro-hardness of the modified textured cemented carbide, prepared under this specific laser energy density, increases by 35 %, while the average friction force decreases by 13.1 %. This improvement is attributed to the grain refinement of the modified textured surface, which induces a fine-grain strengthening effect (Xing et al., 2024). The increase in grain boundary density effectively inhibits dislocation motion under external stress, thereby enhancing surface hardness, and improving friction and wear resistance (Zemlik et al., 2024). Consequently, during milling, the ball-end milling cutter exhibits superior wear resistance when the rake face contacts the chip, resulting in a marked reduction in the effective average milling force.

In contrast, during the preparation process of traditional textured cemented carbide surfaces, the lack of laser energy absorbed by the cladding powder leads to direct application of laser energy on the matrix surface. This interaction causes the substrate to prematurely enter the microstructural coarsening phase. Consequently, the grain size is larger, and the quantity of hard phases is lower compared to the modified textured cemented carbide surface. Therefore, at an average laser energy density of $70.8\,W\,cm^{-2}$, the rake face of the traditional textured ball-end milling cutter exhibits poor wear resistance, which correlates to a higher effective average milling force during the milling process.

A comparative analysis of Fig. 4a and b reveals that the effective average milling forces of both modified and traditional textured cutters decrease significantly after the deposition of the AlCrN coating. The AlCrN coating enhances surface hardness, wear resistance, and high-temperature stability by introducing aluminum into the CrN matrix. During the cutting process, the surface aluminum readily oxidizes to form a dense Al_2O_3 oxide film, which acts as a protective barrier against chemical reactions between the tool, the workpiece, and the environment (Chen et al., 2023). Furthermore, the low thermal conductivity of the coating inhibits oxygen diffusion, thereby further improving the high-temperature milling performance of the ball-end milling cutter.

Figure 5a and b demonstrate that fluctuations in the effective milling force of the modified textured cemented carbide ball-end milling cutter, irrespective of coating presence, remain minimal, indicating robust cutting stability. This stability can primarily be attributed to two factors.

First, the laser-cladding-based preparation of the modified textured surface significantly reduces the occurrence of cracks and pores, thereby minimizing transient vibrations caused by localized fractures within the recast layer during cutting. As illustrated in Fig. 6, the fine-grained carbide particles within the cladding material contribute to grain refinement strengthening of the cladding layer, resulting in a stable and reinforced microstructure. This enhancement improves both the strength and toughness of the cladding layer, effectively preventing the detachment of hard phases from the substrate and thereby increasing the overall surface stability of the tool.

Second, the deposition of the AlCrN coating facilitates the formation of a dense Al_2O_3 oxide film through the reaction of aluminum with atmospheric oxygen during frictional contact. This oxide film possesses a high melting point and exhibits excellent solid lubrication properties, characterized by a low friction coefficient. Under high-speed cutting conditions, the chip rake face maintains superior thermal resistance and efficient chip evacuation (Liu et al., 2024). The surface of the modified textured coating contains a hard phase identified as $TiN_{0.3}$. Following repeated sliding friction, localized detachment of some hard-phase particles occurs, resulting in the formation of small free hard particles. These detached particles are no longer integrated in the continuous coating structure and function as a "third body" at the tool–chip contact interface, serving roles in load bearing and isolation. Tribological investigations have demonstrated that these third-body particles can alter the nature of the interface contact through sliding, rolling, or a combination of sliding-rolling motions under conditions of high contact stress. This behavior mitigates direct sliding contact to a certain degree, thereby reducing frictional resistance at the interface. Specifically, the particles roll in conjunction with the relative sliding motion in the chip contact area (Li and Heß, 2024), effectively transforming the frictional interaction from sliding friction to rolling friction. Compared to sliding friction, rolling friction significantly reduces frictional resistance and vibration, thereby enhancing the operational stability of the

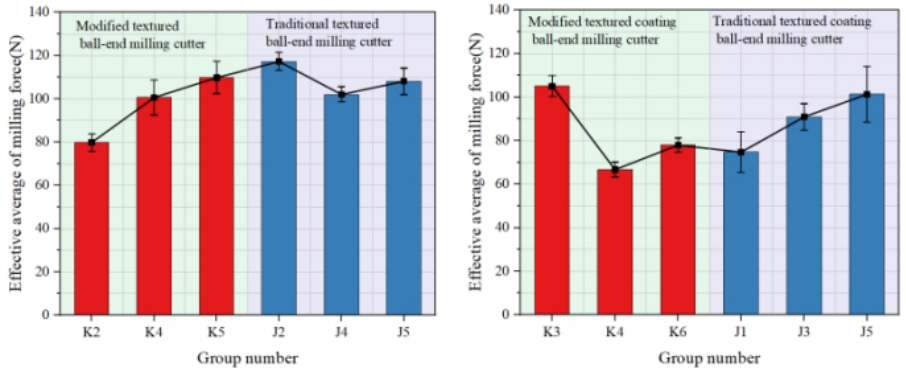

Figure 4. The variation trend of the effective average milling force of the coated modified textured ball-end milling cutter with the number of cutting times. **(a)** Effective average milling force of uncoated ball-end milling cutter. **(b)** Effective average milling force of coated ball-end milling cutter.

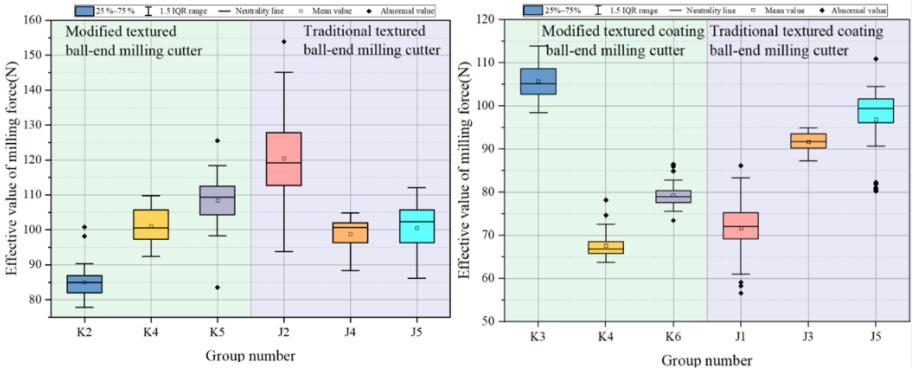

Figure 5. The effective value box diagram of milling force of coated modified textured ball-end milling cutter. **(a)** Effective average box plot of milling force of uncoated ball-end milling cutter. **(b)** Effective average box plot of milling force of coated ball-end milling cutter.

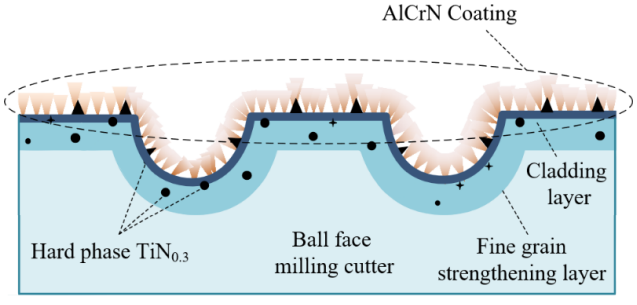

Figure 6. Surface hardening principle of modified textured coating tool.

modified textured coating ball-end milling cutter during machining.

The acquired vibration signals were subjected to denoising using the wavelet transform technique, followed by time-frequency analysis employing the short-time Fourier transform (STFT) (Tong and Wang, 2023). As illustrated in Fig. 7, a comparative examination of the cutting force distribution alongside the vibration time-frequency signal reveals that both the conventional textured tool and the modified textured tool exhibit pronounced nonlinear dynamic responses during machining. The time-frequency representation of the vibration signals demonstrates notable broadband characteristics accompanied by prominent high-energy peaks, indicative of substantial dispersion. Conversely, the cutting stability associated with the traditional textured coated tool displays a transitional distribution pattern overall, with the high-frequency noise in the time-frequency diagram converging. This observation suggests that the coating applied to the tool surface effectively reduces the friction coefficient at the tool–chip interface, thereby mitigating the generation of high-frequency vibrations to some extent. In comparison to the aforementioned tools, the modified textured coated tool demonstrates superior machining stability throughout the process. Specifically, the K4 group not only achieves the lowest maximum vibration energy but also exhibits a distinctly discrete narrow-band background in its spectral profile. This synergistic interaction between the highly concentrated low-modified texture and the coating facilitates a combined effect of friction reduction and vibration suppression. Consequently, it inhibits high-frequency impacts during ma-

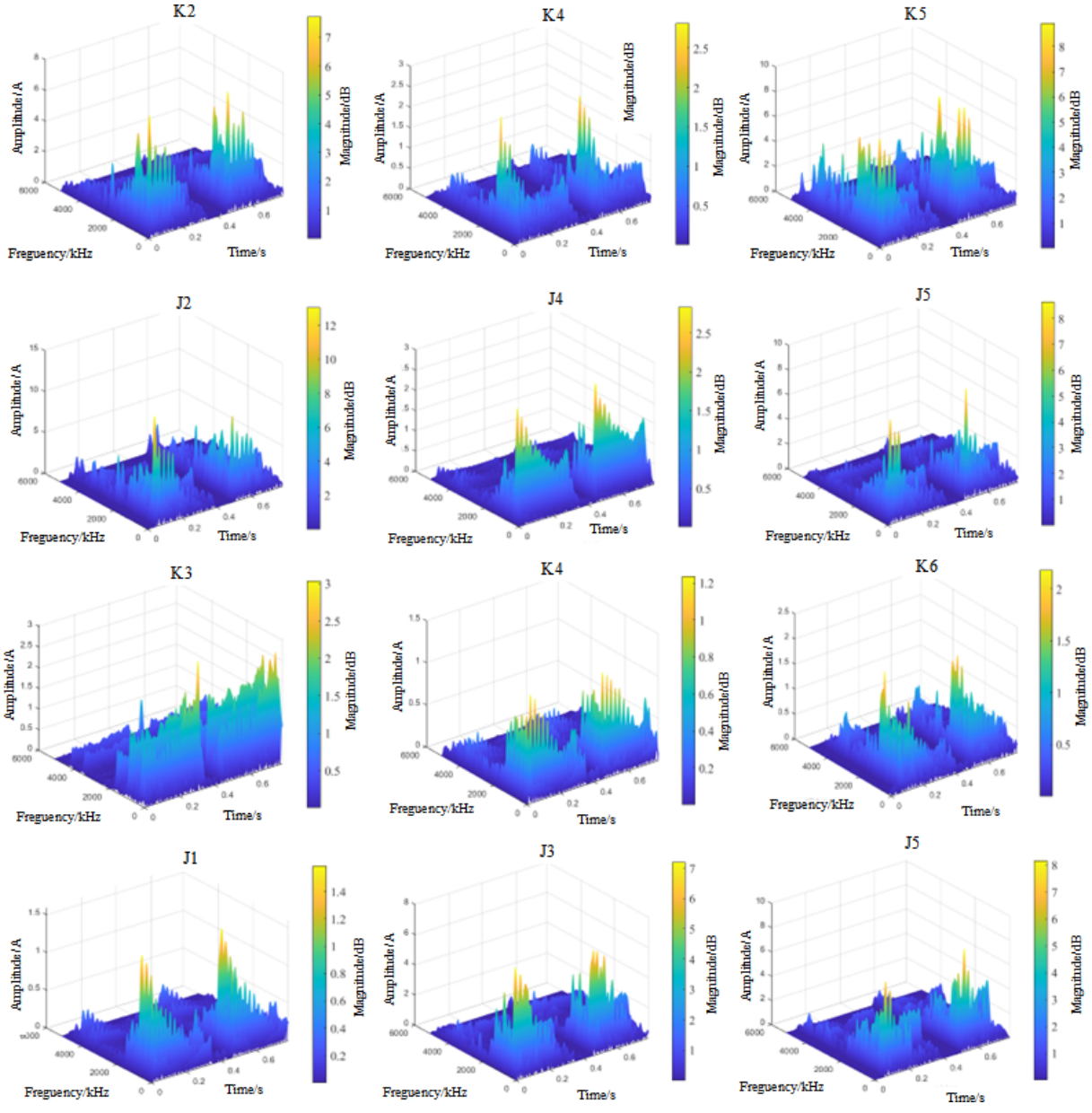

Figure 7. Vibration STFT three-dimensional diagram.

chining, transforming the inherently nonlinear cutting process characterized by high energy and strong fluctuations into a stable machining state marked by reduced cutting forces.

3.2 Analysis of wear results of ball-end milling cutter with textured coating on cemented carbide surface

The surface of conventional textured tools exhibits distinct adhesion layers and wear grooves aligned with the chip flow direction, suggesting that the predominant wear mechanism arises from the combined effects of adhesive and abrasive wear. In comparison, the modified textured surfaces demonstrate enhanced resistance to both adhesive and abrasive wear. The strength and toughness of the cladding layer are enhanced, effectively inhibiting the initiation of abrasive wear and mitigating the extent of adhesive wear. Moreover, this modification prevents the detachment of hard phases from the substrate, thereby significantly improving the overall wear resistance (Xing et al., 2024; Zhu, 2021). As demonstrated in Fig. 8a, a comparison of the rake face wear between the modified textured and traditional textured cemented carbide ball-end milling cutters indicates that the modified textured cutters exhibit significantly reduced wear. This enhancement is primarily attributed to the formation of strengthening phases, such as carbon-deficient W_2C

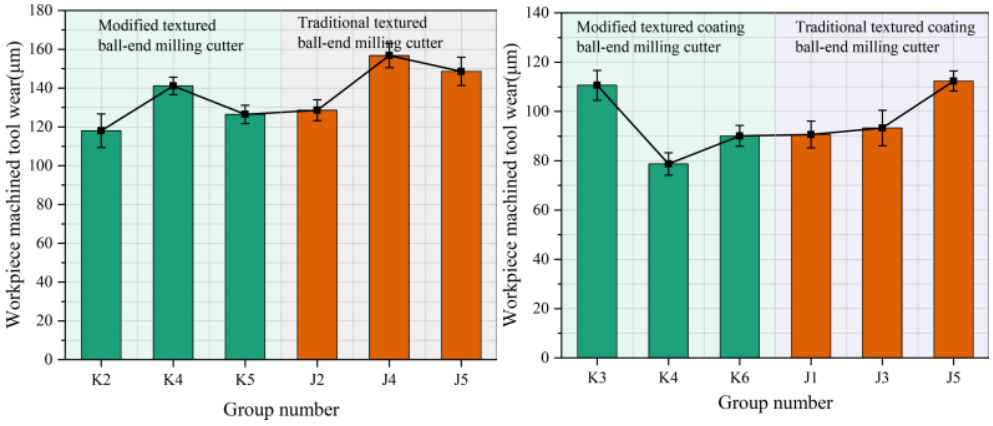

Figure 8. Wear amount of rake face of textured ball-end milling cutter with or without coating modification. **(a)** Wear amount of uncoated ball-end milling cutter rake face. **(b)** Wear amount of coated ball-end milling cutter rake face.

and titanium-nitrogen compounds within the cladding layer. These phases create a pinning effect that inhibits crack propagation. Additionally, the solid solution phase $(Ti,W)C_{1-x}$ contributes to a dispersion-strengthening effect, thereby enhancing the hardness of the recast layer and minimizing microstructural defects. During the wear process, the recast layer of the modified textured surface maintains point-to-surface contact with the titanium alloy workpiece, ensuring a more stable frictional process and delaying the complete wear-through of the cladding layer.

Furthermore, compared to traditional textured surfaces, the strengthened layer of the modified texture contains a higher concentration of hard phases, including TiN, Ti_2N, and $(Ti,W)C_{1-x}$. As the chip slides across the strengthening layer, these hard phases effectively reduce the material removal rate, suppress spalling and plastic deformation, and maintain surface integrity. As wear progresses, a small portion of these hard phases detaches and acts as rolling particles in the contact interface, transforming sliding friction into rolling friction. This transition leads to a decreased friction coefficient and extends the durability of the strengthening layer. In contrast, the strengthening layer of the traditional textured ball-end milling cutter has lower hardness and reduced hard-phase content, resulting in premature wear and early exposure of the tool substrate, which subsequently contacts the chip. The modified textured tool, due to its higher hard-phase content, delays the onset of wear-induced shedding and prolongs the functional lifespan of the strengthening layer, thereby postponing substrate exposure. Consequently, under equivalent cutting durations, the cumulative wear observed in traditional textured tools is significantly greater than that in modified textured tools.

As shown in Fig. 8b, both the modified and traditional textured ball-end milling cutters demonstrate further reductions in rake face wear after the deposition of the AlCrN coating. This enhancement is attributed to the formation of a dense composite oxide layer consisting of Al_2O_3 and Cr_2O_3 at elevated temperatures, resulting from the interaction between aluminum and chromium elements. The composite oxide film exhibits excellent wear resistance, oxidation resistance, and chemical stability, effectively preventing tool–chip reactions and reducing heat diffusion into the substrate. Consequently, the coating significantly enhances the overall wear resistance of the tool. Additionally, the modified textured coating surface exhibits a higher density of molten spatters and fine, hard particles, which act as nucleation cores during the deposition of AlCrN. These nucleation sites facilitate grain refinement, leading to smaller grain sizes and a denser microstructure of the coating. The refined and compact structure of the coating further enhances the adhesion strength and wear resistance at the tool–chip interface, thereby improving the durability and stability of the modified textured coated ball-end milling cutter.

3.3 Analysis of machined surface roughness results

Figure 9a compares the machined surface roughness of cemented carbide modified textured and traditional textured ball-end milling cutters after milling titanium alloy. The results indicate that the surface roughness achieved with the modified textured ball-end milling cutter is significantly lower than that of the traditional textured cutter. This enhancement can be attributed to the higher micro-hardness and the increased presence of hard phases on the surface of the modified textured tool. Its superior wear resistance effectively mitigates the wear-induced passivation of the cutting edge during machining, thereby preserving a sharp cutting edge profile, and reducing both cutting vibration and material adhesion. Under identical cutting durations, the modified textured ball-end milling cutter demonstrates enhanced cutting performance, which contributes positively to the improvement of the machined surface roughness of the titanium alloy.

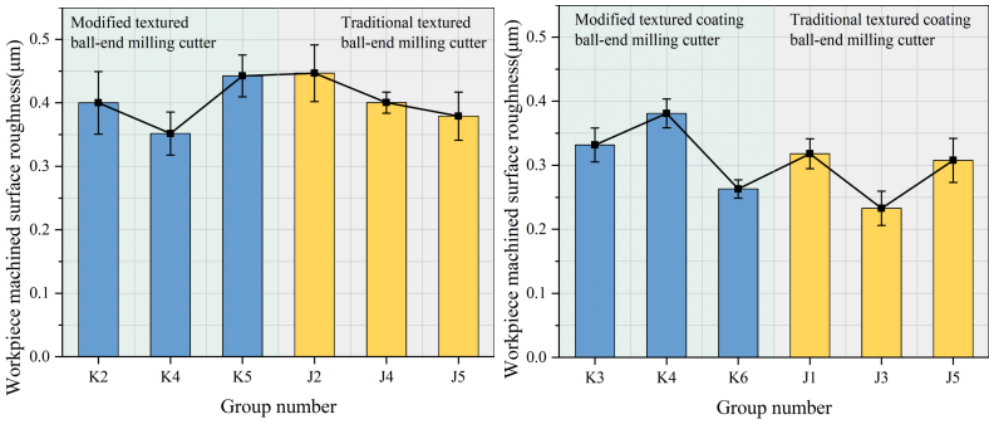

Figure 9. Surface roughness of titanium alloy milled by coated modified textured ball-end milling cutter. **(a)** Surface roughness of titanium alloy milling by uncoated ball-end milling cutter. **(b)** Milling surface roughness of titanium alloy with coated ball-end milling cutter.

Research has demonstrated that during the milling of titanium alloys, cutting vibrations constitute a significant factor influencing the surface roughness of the machined workpiece. Moreover, fluctuations in the effective value of the cutting force have been identified as a primary cause of variations in cutting vibration. In this study, the cutting force signal is utilized as an indirect indicator to assess the trend of cutting vibrations, thereby obviating the need for accelerometers, other vibration sensors, or direct measurement of vibration amplitude (Wang et al., 2022). Experimental results reveal that at average laser energy densities of 70.8 and 75.2 W cm^{-2}, the effective average milling force of the modified textured ball-end milling cutter exhibits minimal fluctuation with respect to the number of cutting cycles, indicating a stable cutting process. However, an increase in the average laser energy density to 108.3 W cm^{-2} results in more significant fluctuations in the effective mean milling force, leading to a marked increase in the machined surface roughness of the titanium alloy. Under the same conditions (70.8 W cm^{-2}), the traditional textured ball-end milling cutter displays similar instability.

Figure 9b compares the machined surface roughness of cemented carbide modified textured and traditional textured coated ball-end milling cutters used for milling titanium alloys. It is observed that the machined surface roughness of both types of milling cutters is reduced. This improvement is attributed to the deposited coating, which significantly enhances the surface adhesion of the tool, minimizes the adhesion between the workpiece material and the tool surface, and mitigates the formation of the built-up edge. The built-up edge tends to detach periodically during machining and re-enter the cutting zone, causing scratches and scales on the machined surface. Therefore, coating deposition effectively contributes to enhancing the surface finish of titanium alloys.

Furthermore, the matrix grain size of the modified textured tool is slightly reduced, and the coating deposited on this fine-grained substrate exhibits increased internal stress and enhanced interfacial bonding strength, thereby improving the elastic modulus of the coating. Meanwhile, the surface roughness of the modified texture, fabricated by laser cladding, is optimized, which further strengthens the coating adhesion. An analysis of the coating H/E ratio (hardness-to-elastic modulus ratio) reveals that the modified textured coating shows a noticeable improvement compared to the traditional textured coating. A higher H/E ratio corresponds to better fracture toughness, greater resistance to plastic deformation, and effective inhibition of crack propagation. The synergistic effect of high hardness and low elastic modulus enables the coating to better resist wear and plastic deformation (Shanmugasundar et al., 2024). This index serves as an important indicator of coating wear resistance, further enhancing the surface performance of the ball-end milling cutter and facilitating the machining of titanium alloy surfaces with lower surface roughness.

4 Conclusions

The milling force exerted by the modified textured ball-end milling cutter during the machining of titanium alloy is significantly lower than that observed with the conventional textured ball-end milling cutter. This reduction can be attributed to the reduced presence of cracks and pores on the surface of the modified textured tool, which decreases the likelihood of vibrations during the cutting process. Furthermore, the carbide particles embedded in the cladding material contribute to the fine-grain strengthening of the cladding layer's microstructure, thereby establishing a reinforced layer that inhibits the detachment of hard phases from the substrate. Consequently, the tool surface exhibits enhanced hardness alongside improved frictional and wear properties, collectively resulting in a decreased effective average milling force.

After the deposition of the AlCrN coating, a hard-phase $TiN_{0.3}$ forms on the tool surface. During multiple sliding friction cycles, this hard phase detaches as hard particles,

which transforms the contact mode from sliding to rolling friction. This transition stabilizes the cutting process and reduces overall fluctuations. Furthermore, the aluminum (Al) element in the coating oxidizes at elevated temperatures, forming an Al_2O_3 oxide film. Due to its high melting point, excellent solid lubrication properties, and low friction coefficient, this oxide film maintains high-temperature stability and facilitates chip evacuation in the contact zone between the chip and the rake face under high-speed cutting conditions, significantly enhancing the milling performance of the ball-end milling cutter.

Compared to traditional textured ball-end milling cutters, the rake face wear of the modified textured cutter is significantly reduced during the machining of titanium alloys. The solid solution phase present on the modified textured surface enhances the cladding layer, increases the hardness of the recast layer, and minimizes structural defects, thereby delaying wear progression. Furthermore, the high hard-phase content in the strengthening layer enables the detached hard particles to function as rolling elements, which reduces the friction coefficient and extends the service life of the strengthening layer. This mechanism effectively delays the exposure of the tool substrate and mitigates rake face wear. Under high-temperature cutting conditions, the aluminum (Al) and chromium (Cr) elements in the coating form a dense oxide layer that provides effective protection to the tool substrate. Additionally, molten spatters on the modified textured surface encourage grain nucleation during coating deposition, refine the grain size, and produce a denser coating microstructure, thereby enhancing wear resistance at the tool–chip interface.

The surface roughness of titanium alloy machined with the modified textured ball-end milling cutter is significantly lower than that achieved with traditional textured tools. This improvement is attributed to the higher surface microhardness and greater hard-phase content of the modified textured tool. The enhanced wear resistance effectively suppresses edge passivation during cutting, which reduces both cutting vibration and material adhesion, thereby improving the quality of the machined surface. Furthermore, the deposited coating minimizes adhesion between the workpiece material and the tool surface, inhibiting the formation of built-up edges. Meanwhile, the improved fracture toughness and resistance to plastic deformation of the modified textured coating effectively prevent crack propagation, allowing the tool to machine titanium alloy surfaces with lower roughness values.

The combined influence of modified micro-texture and AlCrN coating, fabricated via laser cladding technology, can effectively regulate cutting force, enhance cutting stability, and reduce tool wear without altering the macroscopic geometric parameters of the cutting tool. This modification technique demonstrates strong engineering applicability under dry cutting conditions and offers valuable insights for the stable machining of difficult-to-cut materials as well as the design of milling tools aimed at achieving high surface integrity.

Data availability. Data will be made available on request.

Supplement. The supplement related to this article is available online at https://doi.org/10.5194/ms-17-415-2026-supplement.

Author contributions. Conceptualization: SC.Y. and X.T. Methodology: Z.N. Validation: Z.N. and SC.Y. Formal analysis: SC.Y. Investigation: SW.X and X.T. Resources: Z.N. Writing (original draft preparation): SC.Y. Writing (review and editing): SW.X and X.T. Funding acquisition: X.T. and Z.N. All authors have read and agreed to the published version of the paper.

Competing interests. The contact author has declared that none of the authors has any competing interests.

Disclaimer. Publisher's note: Copernicus Publications remains neutral with regard to jurisdictional claims made in the text, published maps, institutional affiliations, or any other geographical representation in this paper. The authors bear the ultimate responsibility for providing appropriate place names. Views expressed in the text are those of the authors and do not necessarily reflect the views of the publisher.

Financial support. This work was supported by the National Natural Science Foundation of China (grant no. 52475445).

Review statement. This paper was edited by Jeong Hoon Ko and reviewed by Fei Zhou and one anonymous referee.

References

Chen, Y., Xu, Y. X., Zhang, H. Q., Wang, Q. M., Wei, T. F., Zhang, F. G., and Kim, K.: Improving high-temperature wear resistance of arc-evaporated AlCrN coatings by Mo alloying, Surf. Coat. Tech., 456, https://doi.org/10.1016/J.SURFCOAT.2023.129253, 2023.

Huang, A., Liu, Y. L., Liu, J. G., Yang, S. P., and Huang, J. G.: Optimization of Process Parameters for Laser Cladding of AlCoCrFeNi High-Entropy Alloy Coating Based on the Taguchi-Grey Relational Analysis, Materials, 18, 4463–4463, https://doi.org/10.3390/MA18194463, 2025.

Jie, M., Qi, Z. X., and Ma, T. F.: Research on the structure and properties of Ni-based alloy coated with laser cladding of cold work mold steel, Journal of Jilin Institute of Chemical Technology, 39, 75–78, https://doi.org/10.16039/j.cnki.cn22-1249.2022.11.015, 2022.

Meng, R.: Study on the effect of laser texture pretreatment on the performance of AlCrN coating on the surface of the matrix, Shandong University, https://doi.org/10.27272/d.cnki.gshdu.2022.007073, 2022.

Ni, X. Y., Zhou, X. L., Huang, H., Ying, C. H., Wu, J. Z., and Liu, X. X.: Research on the design and wear resistance of TC4 titanium alloy surface laser cladding FeCrNiCuSi$_x$ coating, Progress in Laser and Optoelectronics, 1–23, https://link.cnki.net/urlid/31.1690.tn.20251009.1717.018 (last access: 10 October 2025), 2025.

Liang, H., Liu, J. H., Sun, L. K., Hou, J. X., and Cao, Z. Q.: Optimization of the Forming Quality of a Laser-Cladded AlCrFeNiW 0.2High-Entropy Alloy Coating, Coatings, 13, https://doi.org/10.3390/COATINGS13101744, 2023.

Liang, W. Y., Liang, G. X., Dong, L. J., Liu, D. G., and Wang, S. Y.: Microstructure and properties of WC/TiC/Co coating on YG8 cemented carbide surface, Metal Heat Treatment, 46, 168–174, https://doi.org/10.13251/j.issn.0254-6051.2021.12.027, 2021.

Li, H. S., Jiang, M. J., Zhang, C., Yin, J. H., and Zhang, K. D.: Research on cutting performance of laser-textured DLC/-TiAlN composite coating tools, Modern Manufacturing Engineering, 3, 1–8 + 30, https://doi.org/10.16731/j.cnki.1671-3133.2025.03.001, 2025.

Li, Q. and Heß, M.: Experimental Investigation of Frictional Resistance in Sliding Contact between Undulating Surfaces and Third-Body Particles, Machines, 12, https://doi.org/10.3390/MACHINES12030150, 2024.

Li, Q. H., Ma, C. L., Xie, L. T., Wang, B. Z., and Zhang, S. H.: Effect of Coated Composite Micro–Texture Tool on Cutting Shape and Cutting Force during Aluminum Alloy Cutting, Machines, 11, 439, https://doi.org/10.3390/MACHINES11040439, 2023.

Liu, Y. M., Zhang, R., Huang, M. D., and Wang, T. G.: Research status and prospect of AlCrN series tool coatings, Journal of Tianjin Normal University, Natural Science Edition, 44, 1–13, https://doi.org/10.19638/j.issn1671-1114.20240401, 2024.

Li, Y. F., Zhang, J., Huang, X. H., Liu, J., Deng, L. J., and Han, P. Y.: Influence of laser power on microstructure evolution and properties of laser cladded FeNiCoCrMo HEA coatings, Mater. Today Commun., 35, https://doi.org/10.1016/J.MTCOMM.2023.105615, 2023.

Shanmugasundar, G., Vanitha, M., Logesh, K., Cepova L., and Elangovan, M.: Effect of deposition temperature on the tribomechanical properties of nitrogen doped DLC thin film, Front. Mech. Eng., 10, https://doi.org/10.3389/FMECH.2024.1365555, 2024.

Sheng, Z. W., Zhu, H., He, Y., Shao, B., Sheng, Z., and Wang, S. Q.: Tribological Effects of Surface Biomimetic Micro–Nano Textures on Metal Cutting Tools: A Review, Biomimetics, 10, 283–283, https://doi.org/10.3390/BIOMIMETICS10050283, 2025.

Tatsuya, S., Priya, S., and Toshiyuki, E.: Development of a Cutting Tool with a Textured Surface for Dry Cutting of Aluminum Alloys, International Journal of Automation Technology, 3, 199–203, https://doi.org/10.1016/j.promfg.2017.11.013, 2009.

Tan, J. H., Sun, R. L., Niu, W., Liu, Y. N., and Nao, W. J.: Research status of TC4 alloy laser cladding materials, Material Review, 34, 15132–15137, https://doi.org/10.11896/cldb.19050077, 2020.

Tong, X. and Wang, S. M.: Vibration Analysis Method of Textured Coating Carbide Surface Based on STFT, J. Instrum., 44, 284–295, https://doi.org/10.19650/j.cnki.cjsi.J2210860, 2023.

Tong, X., Han, P., and Yang, S. C.: Study of the friction behavior of AlCrN coated micro-textured surfaces, Tribol. Int., 177, https://doi.org/10.1016/J.TRIBOINT.2022.107985, 2023.

Wang, J. Y., Sun, Y. B., Niu, H. J., and Lin, C. X.: TC4 alloy surface laser cladding CoCrW coating process and properties, Journal of Dalian Maritime University, 49, 117–126, https://doi.org/10.16411/j.cnki.issn1006-7736.2023.01.013, 2023.

Wang, Z. Y., Li, H. Y., and Yu, T. B.: Study on Surface Integrity and Surface Roughness Model of Titanium Alloy TC21 Milling Considering Tool Vibration, Appl. Sci., 12, 4041–4041, https://doi.org/10.3390/APP12084041, 2022.

Wu, X. F., Zhan, J. M., and Mei, S. L.: Optimization of Micro-Texturing Process Parameters of TiAlN Coated Cutting Tools by Femtosecond Laser, Materials, 15, 6519–6519, https://doi.org/10.3390/MA15196519, 2022.

Xing, S., Tong, X., Yang, S. C., and Li, X. Y.: Study on shallow configuration preparation and macroscopic and microscopic properties of cemented carbide surface, Int. J. Refract. Met. H., 122, 106727, https://doi.org/10.1016/J.IJRMHM.2024.106727, 2024.

Zhang, C.: Preparation and application of liquid-phase assisted laser textured DLC/TiAlN composite coating tools, Soochow University, https://doi.org/10.27351/d.cnki.gszhu.2024.002762, 2024.

Zemlik, M., Białobrzeska, B., Stachowicz, M., and Hanszke, J.: The Influence of Grain Size on the Abrasive Wear Resistance of Hardox 500 Steel, Appl. Sci., 14, 11490–11490, https://doi.org/10.3390/APP142411490, 2024.

Wu, Z., Xing, Y. Q., and Chen, J. S.: Improving the Performance of Micro-Textured Cutting Tools in Dry Milling of Ti-6Al-4V Alloys, Micromachines, 12, 945–945, https://doi.org/10.3390/MI12080945, 2021.

Zhou, Y.: Development and performance of composite textured CrAlN coated tools, Jiangsu University, https://doi.org/10.27170/d.cnki.gjsuu.2022.000572, 2022.

Zhu, J. X.: Research on the microstructure and friction and wear properties of WC and TiC enhanced iron-based composite coatings, Anhui Jianzhu University, https://doi.org/10.27784/d.cnki.gahjz.2021.000359, 2021.